Multi-Decadal Oscillations of the Ocean Active Upper-Layer Heat Content

Vladimir I. Byshev,[1] Victor G. Neiman,[1] Mikhail V. Anisimov,[1] Anatoly V. Gusev,[1,2] Ilya V. Serykh,[1] Alexandra N. Sidorova,[1] Alexander L. Figurkin,[3] and Ivan M. Anisimov[1]

Abstract—Spatial patterns in multi-decadal variability in upper ocean heat content for the last 60 years are examined using a numerical model developed at the Institute of Numerical Mathematics of Russia (INM Model) and sea water temperature-salinity data from the World Ocean Database (in: Levitus, NOAA Atlas NESDIS 66, U.S. Wash.: Gov. Printing Office, 2009). Both the model and the observational data show that the heat content of the Active Upper Layer (AUL) in particular regions of the Atlantic, Pacific and Southern oceans have experienced prominent simultaneous variations on multi-decadal (25–35 years) time scales. These variations are compared earlier revealed climatic alternations in the Northern Atlantic region during the last century (Byshev et al. in Doklady Earth Sci 438(2):887–892, 2011). We found that from the middle of 1970s to the end of 1990s the AUL heat content decreased in several oceanic regions, while the mean surface temperature increased on Northern Hemisphere continents according to IPCC (in: Stocker et al. Contribution of working group I to the fifth assessment report of the intergovernmental panel on climate change, Cambridge University Press, Cambridge, 2013). This means that the climate-forcing effect of the ocean–atmosphere interaction in certain energy-active areas determines not only local climatic processes, but also have an influence on global-scale climate phenomena. Here we show that specific regional features of the AUL thermal structure are in a good agreement with climatic conditions on the adjacent continents. Further, the ocean AUL in the five distinctive regions identified in our study have resumed warming in the first decade of this century. By analogy inference from previous climate scenarios, this may signal the onset of more continental climate over mainlands.

Key words: Heat content, active upper layer, temperature, ocean, atmosphere, convection, climate change, multi-decadal variability, climatic scenarios.

1. Introduction

The global ocean is the most significant and energetic heat accumulator in the global climate system and the current trend of increasing mean near-surface air temperature is the most widely recognized signal of recent, short-term climate variability (IPCC 2007, 2013). In addition to this trend, however, there are also intense, climatic oscillations identified within various-scales of global oceanographic and meteorological fields (Chu 2011; de Viron et al. 2013; Steinman et al. 2015) that are attracting attention in various applications (e.g., Bond et al. 2003; Knight et al. 2006; Akasofu 2010; Chambers et al. 2012; Abraham et al. 2013; Liu and Sui 2014). Furthermore, there is evidence that climatic signals in the temperature and precipitation fields extant over the continents and oceanic areas appeared to be in anti-phase during the last century (Byshev et al. 2006; Noake et al. 2012).

Figure 1a–g shows variability of the average annual anomalies of the near-surface air temperature during the 20th century in several key areas of the Northern Hemisphere. Interannual (periods of 2–8 years) and multi-decadal (periods of 20–50 years) quasi-cyclic oscillations superimposed on the secular nonlinear trend are easily identifiable in the figure. It is also clearly seen that the shapes of the air temperature secular nonlinear trends over the oceans (Fig. 1b, e) and the continents (Fig. 1d, f, g) are reversed. This means that, in the first half of past century, the air temperature grew faster over the oceans in comparison with the continents, accompanied by a mild temperature decrease in some continental areas (Fig. 1d, f). In the second half of the 20th century, the air temperature resumed its' growth

[1] P.P. Shirshov Institute of Oceanology, Russian Academy of Sciences, 36 Nakhimovsky Pr., Moscow 117997, Russia. E-mail: labbyshev@ocean.ru; anatoly.v.gusev@gmail.com
[2] Institute of Numerical Mathematics, Russian Academy of Sciences, 8 Gubkina St., Moscow 119901, Russia.
[3] Pacific Researches and Fisheries Centre, 4 Shevchenko, Vladivostok 690091, Russia. E-mail: figurkin@tinro.ru
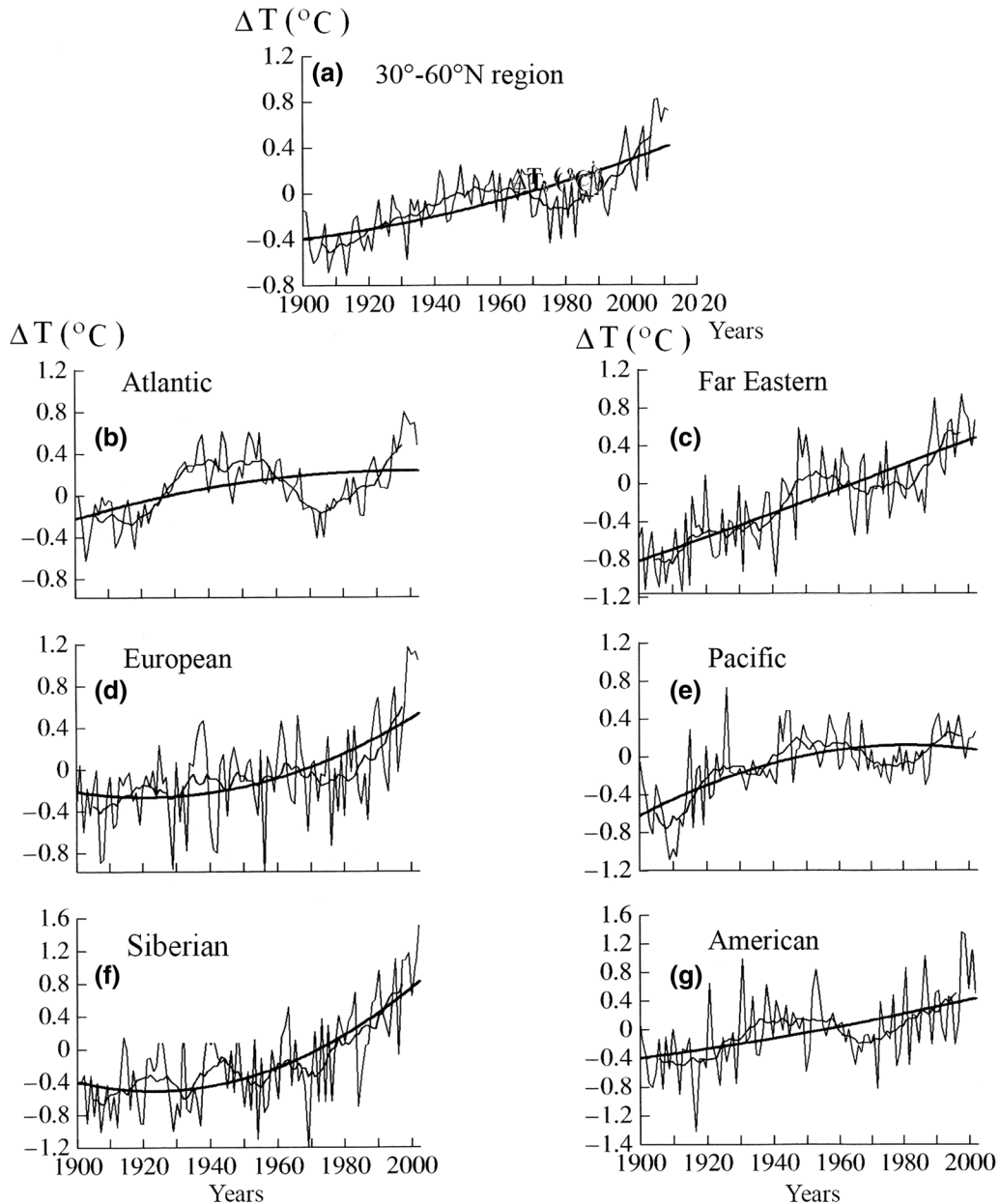
Figure 1
Near-surface air temperature anomalies for the period from 1900 to 2002: averaged for the area between 30°N and 60°N, **a** the entire area, and for particular regions: **b** Atlantic (60°W–0°), (c) Far Eastern (120°E–170°E), **d** European (0°–60°E), **e** Pacific (170°E–120°W), **f** Siberian (60°E–120°E), and **g** American (120°W–60°W). The data are from Climatic Research Unit, University of East Anglia (http://www.cru.uea.ac.uk/cru/data/temperature/). Thin curves represent the original data, semi-bold curves—the 11-year sliding means, bold curves—the nonlinear trends of second order; vertical (ordinate) scale–temperature anomalies

over the continents contrary to the oceanic areas, where temperature growth was dampened.

At the same time, Fig. 1 shows that in the American and Far Eastern sectors (Fig. 1c, g), as well

as in the region as a whole (Fig. 1a), the secular trend of the anomaly of the near-surface temperature was predominantly linear. Such a situation could mean that the temperature fluctuations in the oceanic

regions were most selectively reflected in the thermal regime of the Euro-Asian continental region. At the same time, climatic conditions in the American and Far Eastern regions, as well as the corresponding average characteristics of the region under investigation as a whole, were much less affected by the influence of this factor.

Figure 2 shows that the linear trend does not unequivocally reflect the nature of the global intra-century variability of the temperature of near-surface air in the Northern hemisphere. Our refinement of this character with the help of the calculation of the nonlinear trend shows once again that in the significant areas of the Atlantic and Pacific oceans the temperature regime in the 20th century was somewhat different in comparison with the continents. The regions of negative values of the nonlinear trend above the oceans (shown in blue in Fig. 2b) reveal a

slowdown or even interruptions in the course of the known global warming on mainland. It seems again that this type of thermal regime of the atmosphere over the ocean is directly related to the processes of internal redistribution of thermal energy within the global climate system. It is obvious that during these processes the phases of heat accumulation and thermal pumping in the ocean and in the atmosphere have mutually opposite signs, that was discovered by us and shown in Figs. 1 and 2.

Consequently, there is reason to believe that this characteristic of climatic variability in the ocean and atmosphere is a result quasi-periodic heat redistribution within the global climatic system (Li and Luo 2013; Liu and Sui 2014; Mann et al. 2014). In fact, statistically significant spectral peaks at the interannual and multi-decadal periods have no other explanation than that they are natural variations of
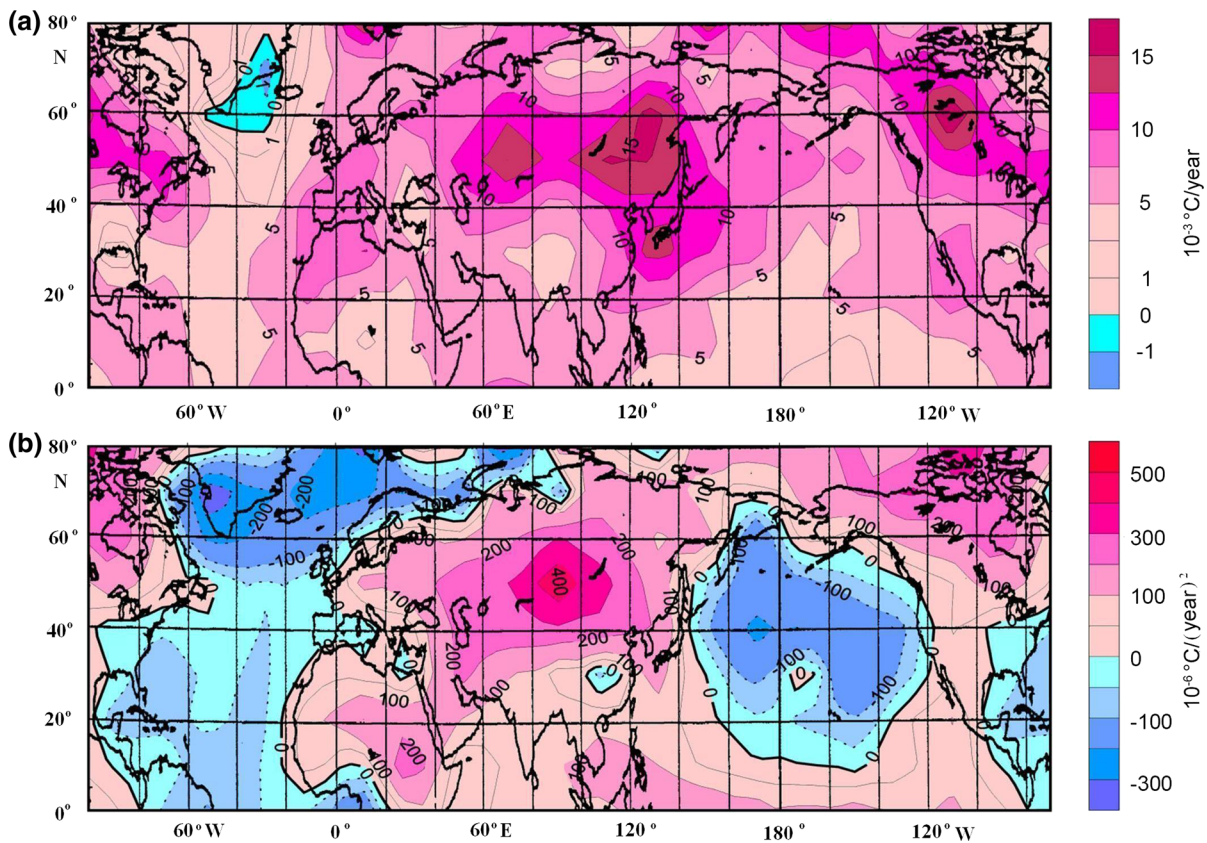

Figure 2
The value of secular trends of the near-surface air temperature anomalies in the Northern Hemisphere in the 20th century: **a** linear trend and **b** quadratic trend

climatic system dynamics reflecting non-stochastic phase states of the global climate (Mokhov et al. 2008; Wouters et al. 2012). By analogy with numerical modeling terminology, such periodically interchanging multi-decadal stages of the climatic system may be called "climate scenarios".

This inherent phase structure in climate variability is revealed by relatively steady episodes (25–35 years) of amplification and attenuation of specific "marine" and "continental" climate symptoms in Europe and North-western Asia observed during the last 100 years (Byshev et al. 2011). Some of this episodes were marked by accompanying changes in river discharge, variations of the sea level (e.g., in the Caspian Sea), extreme seasonal air temperatures, and other severe climatic phenomena (Lebedev and Kostianoy 2008; IPCC 2013).

Intra-secular variability of the temperature and pressure fields in the Northern Atlantic region key areas are shown in Fig. 3. Following Byshev et al. (2011), the full set of thermodynamic estimates was subdivided into three, conditionally separated clusters, and each such cluster was then matched with a certain climatic scenario. The duration of each scenario was found to be about 25–35 years, with the
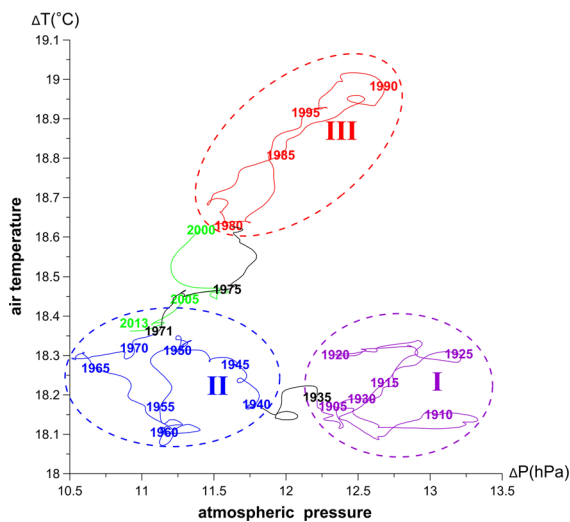

Figure 3

Air temperature vs. atmospheric pressure in the North Atlantic region for the North Atlantic climatic system during 1900–2015 (adapted from Byshev et al. 2011). The horizontal axis represents the sea surface air pressure difference ΔP, and the vertical axis—the near-surface air temperature difference ΔT between Azores High and Island Low

transitions from one scenario to another taking 2–3 years, i.e., the change occurred very quickly. The corresponding fields of hydrometeorological properties in other regions of the Earth were analyzed in a similar way. For example, thermobaric index phase trajectories describing dynamics of the regional climate evolution in Eurasia also revealed three scenarios referred to 1900–2000 with similar time frames. In this case the Siberian anticyclone and the Hindustan Peninsula depression were taken as atmospheric centers of reference. In an earlier independent study Bond et al. (2003), noted a similar phase reconstructions within the sea surface atmospheric pressure field over the North Pacific region. These facts suggest that the short-period intracentennial variability of the climate scenarios is manifested at the global scale. The time frames of the identified climatic scenarios were then used in this study as a guide for the selection of temporal parameters for the ocean heat content evolution assessment.

Understanding the origin and effects of interannual and multi-decadal variations in the oceans and atmosphere is one of the major challenges in climate science. As such, the atmosphere plays a key role in the interannual climatic processes, whereas the ocean is responsible for the longer-period processes (Monin 1986; Gulev et al. 2013; Gulev and Latif 2015). In this respect, the positive secular trend in ocean heat content is generally recognized as the main feature of global climate changes (Levitus et al. 2009; Liman et al. 2010; IPCC 2013). At the same time, however, there are certain regions in the North Atlantic and North Pacific (Byshev et al. 2009) where the Active Upper Layer (AUL) has undergone a loss of its heat content during the period 1975–2000.

The thermal characteristics of the AUL are determined mainly by air-sea interaction processes. AUL thickness, for example, depends both on whether the wind-field drives convergent or divergent ocean flows, and on the intensity of the vertical convection (Gill 1982). The deepest convection occurs in areas of the North Atlantic Ocean during the boreal winter, when the AUL lower boundary reaches depths of more than 1000 m (Byshev and Orlov 1993). In contrast with regions in the North Atlantic and Southern Ocean, the deepest seasonal density convection within other areas of the global ocean is

typically restricted to the upper 100–400 m. Therefore, the AUL may be considered as the uppermost ocean layer whose thickness depends on the maximum depth of seasonal vertical density convection (Byshev and Orlov 1993; Byshev et al. 2016a), and represents the most active ocean layer involved in the processes of the ocean–atmosphere exchange.

Additional support for the dominant role the ocean plays in constraining climate variability comes from observations obtained from two large Russian ocean observation programs: MEGAPOLYGON (Pacific ocean, 1987) and ATLANTEX-90 (Atlantic Ocean, 1990) which show intense heat release in several energetically active oceanic zones that occurred in the last quarter of the 20th century (Byshev and Snopkov 1990; Byshev et al. 1993). These observational results were subsequently supported by numerical modeling of the thermohaline circulation in the North Atlantic Ocean (Moshonkin et al. 2004).

Numerous other studies have revealed the multi-decadal phase structure of climate variability (Minobe 1999; Stephens et al. 2001; Bond et al. 2003; Tsonis et al. 2007; Swanson and Tsonis 2009; Wang et al. 2009; Wyatt et al. 2012; Zhang et al. 2012; Watanabe et al. 2014). One of the important findings was a "climatic shift" observed in the mid-1970s by Bond et al. (2003) which we argue coincided with a climatic regime change over the Atlantic region. Lee and McPhaden (2008) presented essential information on the climatic phase variability in the Pacific and Indian Oceans at the beginning of the 21st century. Nakamura (2013) found quasi-simultaneous climatic changes in the Sea of Okhotsk and the Greenland Sea. All these studies provide the evidence that the multi-decadal climate variations are an important feature of the entire climatic system dynamics.

In this study we investigate spatial and temporal characteristics of the multi-decadal climate variability and estimate the interrelationship and mutual correspondence of the oceanic and atmospheric components of this variability.

2. Methods and Data

AUL fields in the northern parts of the Atlantic and Pacific and in the Southern Oceans were analyzed using the global ocean circulation model developed at the Institute of Numerical Mathematics (INM) (Gusev and Dianskiy 2014). Numerical experiments were performed for the period from 1948 to 2007. The model had a horizontal resolution of 0.5° in the meridional and 1° in the zonal direction. For the North Atlantic Ocean, some additional numerical experiments for the period from 1958 to 2006 were done with a higher spatial resolution: 0.25° × 0.25°. The integration time step in these experiments was 1 h. The model estimated the mean long-term seasonal thickness of the Upper Mixed Layer (UML) for the global ocean and the vertical structure of potential temperature, salinity and density, as well as their spatial and temporal evolution for five selected regions in the Atlantic, Pacific and Southern Oceans (identified below). The UML bottom boundary was estimated as the depth of the maximum of the second derivative of the potential density profile. This method accounts the effect of vertical convection, which strongly regulates the seasonal evolution of AUL thermal structure. A detailed description of these numerical experiments is given in (Moshonkin et al. 2004) and (Gusev and Dianskiy 2014).

The INM model is based on 3D primitive ocean dynamics equations with hydrostatic and Boussinesq approximations. Notice, that simultaneous use of these two approximations is a common practice. The model is formulated in the generalized orthogonal coordinates horizontally and terrain-following sigma coordinates vertically. In the model numerical realization the 'splitting method' of physical processes was used (Gusev and Dianskiy 2014). Such approach allows to apply implicit and semi-implicit schemes with a larger time step and to achieve significant advantage in comprehensive computationally intensive experiments.

The verification of the numerical model was done based on the data from large-scale oceanic projects: POLYGON-70 (Kort and Samoylenko 1983), POLYMODE (Atlas POLYMODE 1986), MEGA-POLYGON (Experiment MEGAPOLYGON 1992) and ATLANTEX-90 (Ivanov and Morozov 1991). The heat fluxes, salinity and impulse at the ocean surface taken from CORE (Large and Yager 2004) were used model boundary conditions.
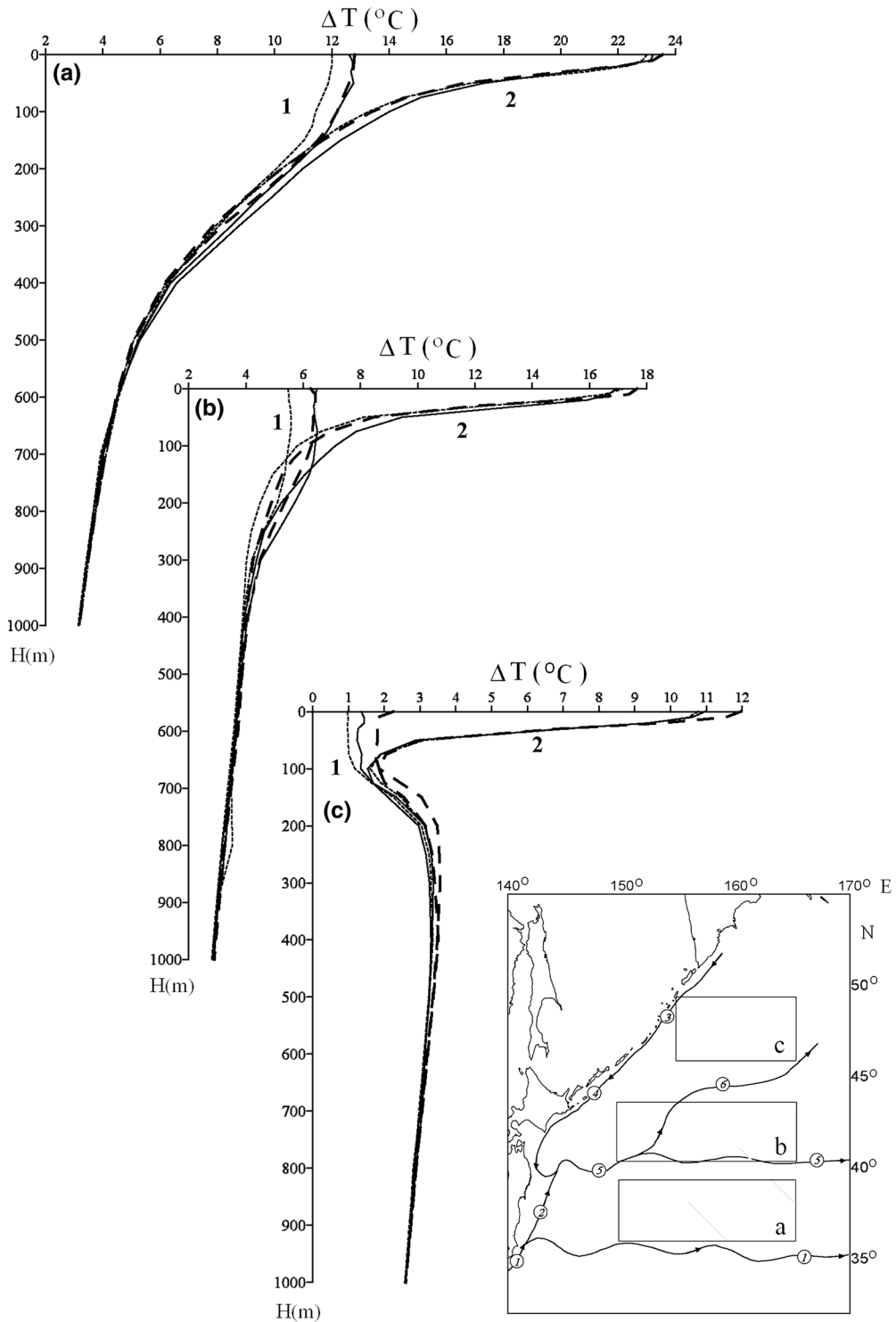
We selected particular ocean regions that give the most unambiguous information on the evolution of the ocean thermal regime at multi-decadal timescales.

Byshev et al. ([2016b](#)) identified of such areas on the basis of the spatial structure of the global interdecadal atmospheric oscillation. In the present study, we

◀Figure 4

Temperature profiles in the upper 1000 m of the North-West Pacific Ocean for cold (*1*) and warm (*2*) seasons in three structural zones: **a** subtropic, **b** intermediate, and **c** subArctic. Temperature profiles are averaged within the time frames of three climate phases: 1960–1974 (*solid curve*), 1975–1999 (*dotted curve*), and 2000–2014 (*dot-dash curve*). The *inset* shows the study area with the schematics of the major currents (*lines with arrows*): *1* main Kuroshio; *2* northern branch of Kuroshio; *3* Kuril Current; *4* Oyashio; *5* Subarctic Current; and *6* northern branch of Subarctic Current

consider the areas of the most active cyclogenesis in the atmosphere as the primary candidates for such regions. We will call these areas the informative regions of the ocean (IRO). Although, according to our preliminary assessment, there is a number of IRO in the global ocean, we have selected five particular regions on the basis of their crucial role in the short-term climatic variability. The following five IRO have been chosen to model the intra-secular evolution of the AUL heat content:

- North Atlantic IRO, bound by 55°N–65°N and, 40°W–30°W, in the North Atlantic Ocean;
- North Pacific IRO, bound by 40°N–45°N, and 152°E–157°E, in the North Pacific Ocean;
- Southern IRO I, bound by 67.5°S–62.5°S, and 45°W–40°W, in the Southern Ocean;
- Southern IRO II, bound by 65°S–60°S, and 72,5°E–77.5°E, in the Southern Ocean;
- Southern IRO III, bound by 55°S–50°S, and 145°E–150°E, in the Southern Ocean.

The first two regions are characterized by the large-scale negative sea surface temperature (SST) anomalies in 1975–1999 (Byshev et al. 2009). The spatial structure and particular values of these anomalies appear to indicate the zones of deep convection (Anisimov et al. 2012) signifying the areas of previously enhanced turbulent sensible and latent heat flux from the ocean into the atmosphere.

To evaluate criteria of climatic sensitivity in the selected regions we considered atmospheric cyclogenesis in the selected IRO. By doing this we take into account the fact that an increase of cloudiness constrains incoming short-wave solar radiation onto the sea surface and reduces the AUL heat content. Additionally, the model was verified against the climate–mean sea water temperature summer and

winter vertical profiles for several areas in the North-West Pacific Ocean bound by coordinates 30°–60°N, and 150°–180°E (Fig. 4, Byshev et al. 2016a).

The profiles were obtained after spatial and temporal averaging of all available observational data. The final data set used for this assessment included 1,048,113 water property profiles, which were obtained in the above area during the period from 1960 to 2015.

As it is seen in Fig. 4a, b, the temperature profiles correspond well with the case of the density-driven convection increase during the climate phase of 1975–1999. Consequently, the ocean heat flux to the atmosphere appeared to have been increasing at that period. At the same time, the AUL heat content in the area was found to have been increasing from 2000 to 2014, evidence of recent heat accumulation in the North-West Pacific Ocean area. If this rate of heat income is maintained at this level, then the AUL heat content in the area will reach the value of 1975 over the next 3–5 years. If so, the ocean state may reach the phase of its next thermal discharge.

3. Results

Interrelation of the multi-decadal climate variability in the North Atlantic region with the AUL parameters and heat content was considered in Anisimov et al. (2012). As the model results confirm, the character of the AUL temporal evolution follows the variations in the ocean–atmosphere heat exchange. This leads to a conclusion that a similar correlation exists not only for individual regions, but also for the global ocean as a whole. The evident seasonal distinction in the large-scale ocean–atmosphere heat exchange is clearly exposed by the winter/summer difference in the global UML topography (Fig. 4). During the boreal winter, the thickness of the upper mixed layer in high and mid latitudes is significantly increased in comparison with the warm season (Fig. 4a). A possible reason for this is intensification of vertical convection in the ocean in the winter period. The general spatial distribution of the UML thickness has a clear anisotropic character meaning that the strongest density convection is confined to distinct oceanic regions, five of which

were specified in this study as the IRO. Herewith, it should be also taken into account that the global scale of a spatial structure of the ocean convection is

depended of climatic factor. At the same time, smaller specific details of this structure, shown on Fig. 5, seem to be determined by the heterogeneity of
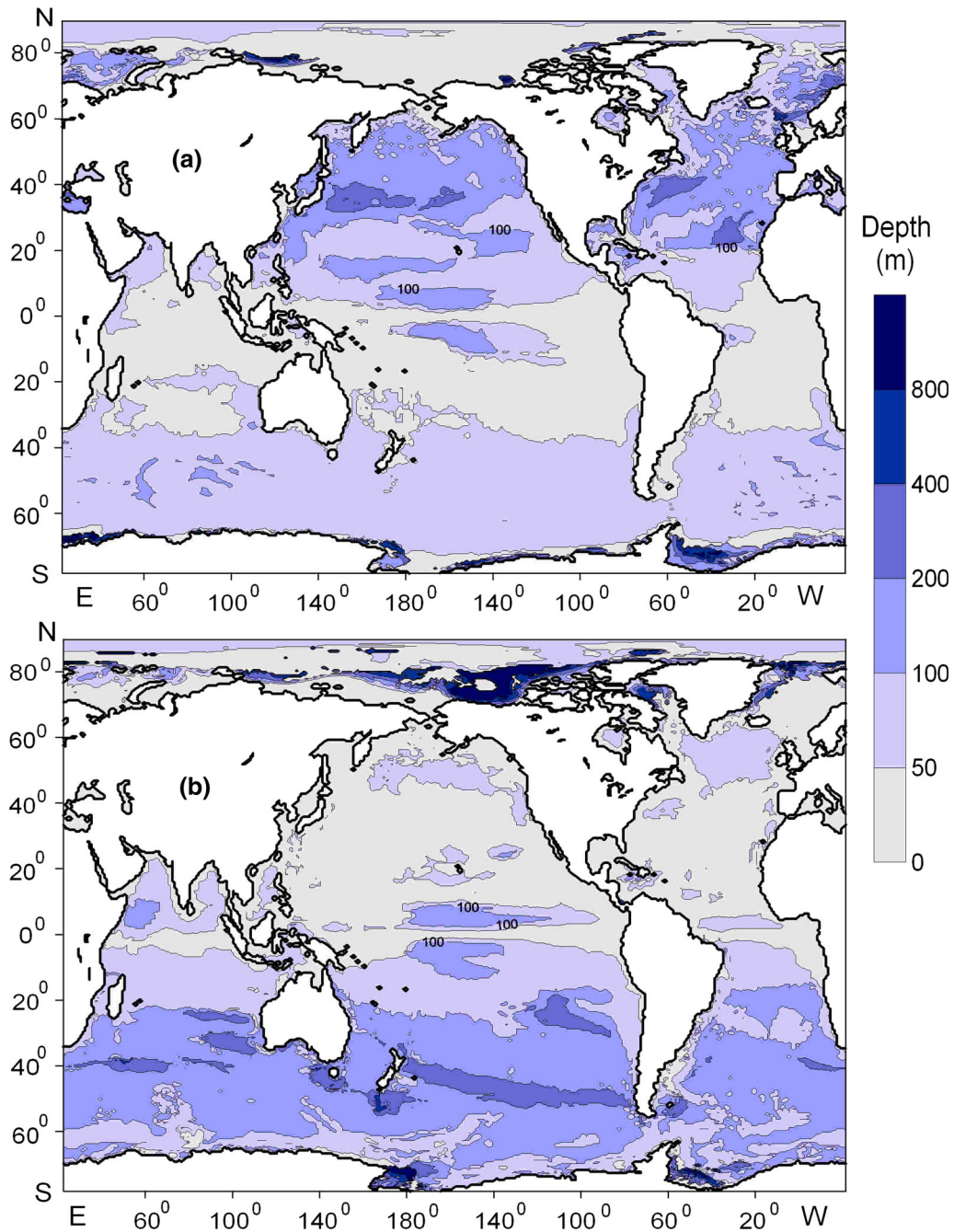

Figure 5
The global topography of the ocean upper mixed layer (UML): **a** mean boreal winter (January–March), and **b** mean boreal summer (July–September)

the temperature field associated with the frontal zones, eddies, current meanders and other oceanic anomalies. Besides, the regional variations in the upper ocean temperature fields are known to be influenced by anomalies of the atmospheric circulation over the ocean; for example, the outbreak and spread of the cold polar and continental air-masses over the oceanic areas.

The results of the temperature structure simulations for the five defined IRO are shown in Figs. 6, 7, 8, 9 and 10. The mean vertical temperature profiles within the upper 800 m indicate both quantitative and qualitative changes of this structure during the second half of the 20th century. Before the mid-1970s, the AUL heat content in the North Atlantic IRO was relatively high (Fig. 6). This means that the layer was accumulating heat during this period. After that, a substantial decrease in the AUL mean temperature

occurred until the beginning of 2000s, when it started increasing once again. The crucial question is thus: What is the source of the AUL heat inflows and outflows over the multi-decadal time scale? A preliminary answer to this question is that the character of the multi-decadal variability in the AUL heat content strongly depends on the fluctuations of the layer thickness, which is determined primarily by wind forcing and the depth of the vertical density convection. This infers a direct link between AUL heat content and its large-scale heat exchange with the atmosphere. Our numerical experiments thus capture the principal oscillation, which we denote as the "Multi-decadal Oscillation of the Heat content in the Ocean" (MOHO).

In addition, simulated variations of the AUL salinity (Fig. 11) and potential density within the studied IRO for the period from 1958 to 2006 were in
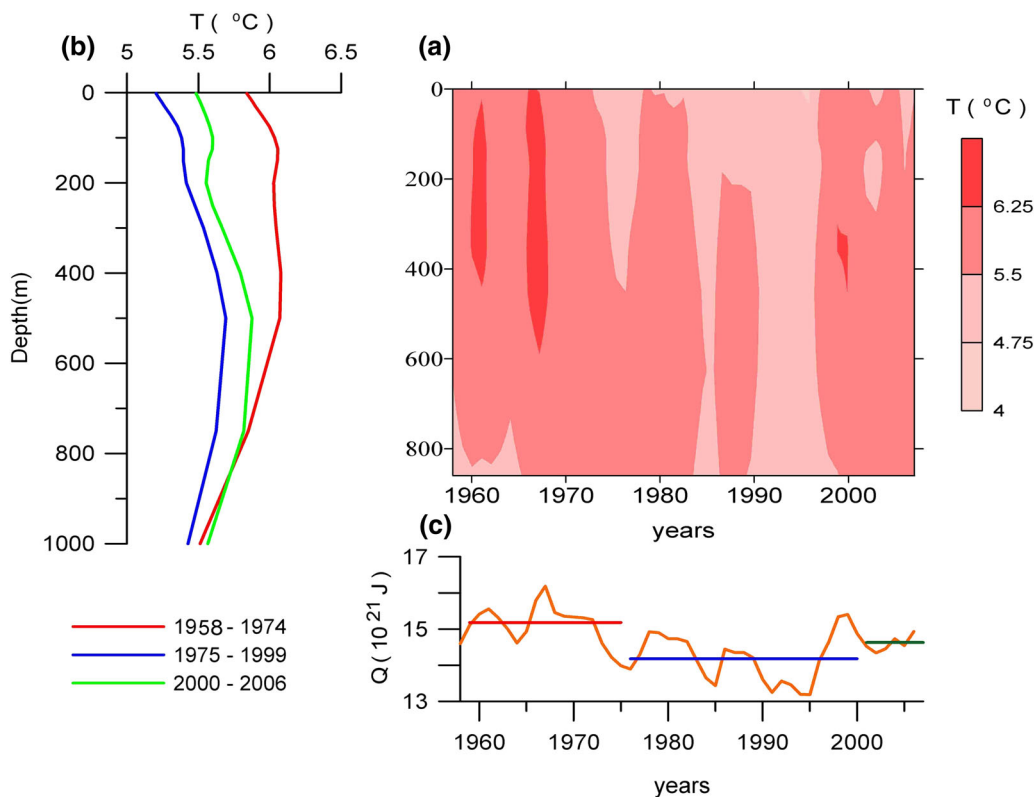

Figure 6
Evolution of the thermal structure of the AUL in the North Atlantic IRO (55°N–65°N, 40°W–30°W): **a** averaged temperature time course for the boreal winter seasons (January–March) from 1958 to 2006; **b** vertical profiles of winter sea water temperature averaged within three climate phases with the time frames specified in the plot, and **c** heat content, Q, within the upper 800-m layer for period of 1958–2006
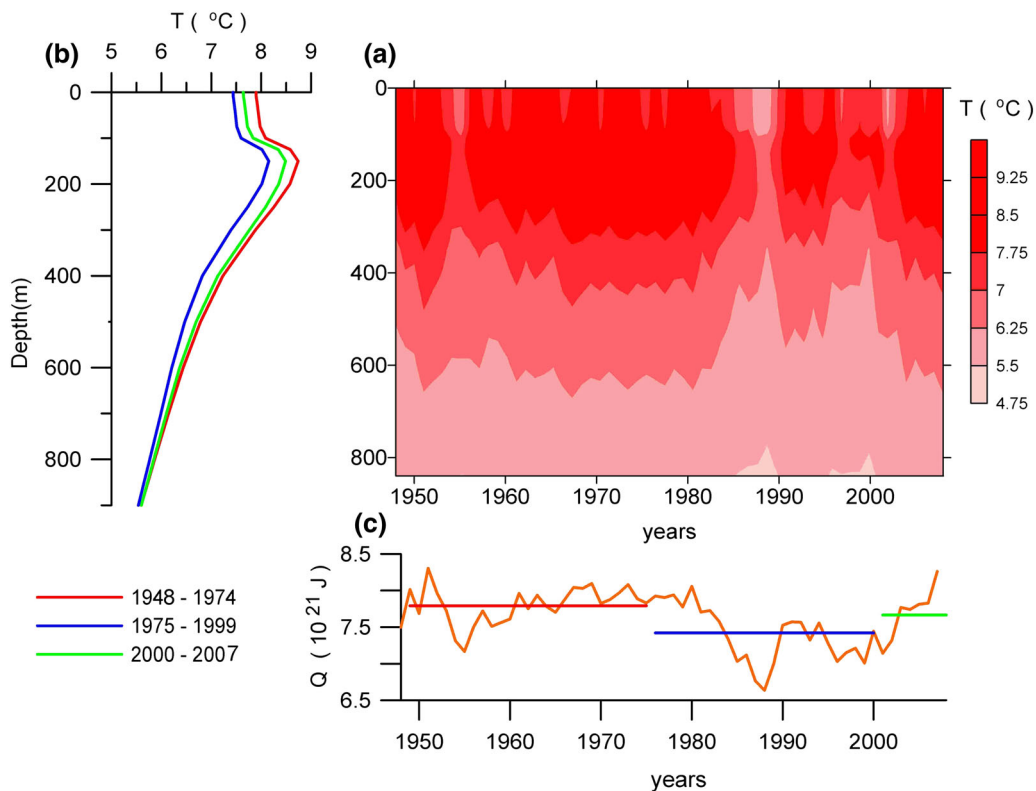
Figure 7
Same as in Fig. 6, but for the North Pacific IRO (40°N–45°N, 152°E–157°E) and for the period from 1948 to 2007

a good agreement with those for the temperature. These five IRO regions are characterized by the periodic formation of cold and dense surface water masses (Figs. 6, 7, 8, 9, 10) (Anisimov et al. 2012). Consequently, the period between mid-1970 s and late 1990s may be considered as the interval of intense deep convection, i.e., the phase of active ocean heat discharge. Entering the atmosphere, the ocean heat is eventually transformed into the energy of cyclones, who, upon reaching the continents, substantially affect their climatic characteristics. In contrast, based on our numerical experiments, we may conclude that before and after this period, the intensity of deep ocean convection in these IRO was diminished.

Similar results were obtained for the central part of the North Pacific Ocean. The AUL in the Pacific IRO warmed up until the mid-1970s (Figs. 4, 7). Following that, there was a relatively long period (∼25 years) of the AUL cooling, replaced by a new

period of the AUL warming from the beginning of the 2000s.

The phases of the MOHO (periodical cycles) are evident in the mean vertical temperature distributions in the upper 600-m layer of water averaged over specific time intervals (Fig. 7b). The intervals were selected based on particular climate phases outlined earlier (Fig. 3) for the Northern Hemisphere (Byshev et al. 2011). Therefore, by comparing the AUL heat content within two IRO, the North Atlantic (0–800 m) and the North Pacific (0–600 m), we can see the similarity in phase structure of their heat accumulation and discharge observed in the last seven decades. A noteworthy result is the remarkable correspondence of the 1975–1999 AUL heat content evolution phase in the North Atlantic and the North Pacific Oceans, which indicates a quasi-simultaneous development of thermodynamic processes in these two oceans. This result agrees with several earlier studies (Minobe 1997; Stephens et al. 2001; Tsonis
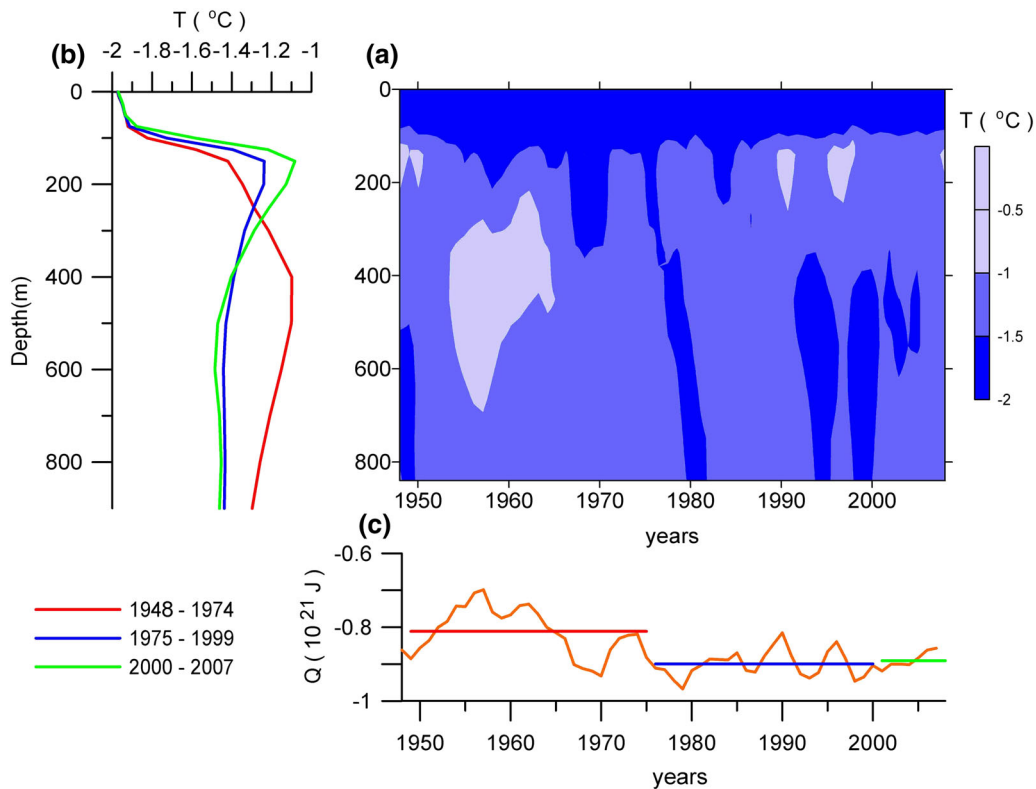
Figure 8
Evolution of the thermal structure of the AUL in the Southern IRO I (67.5°S–62.5°S, 45°W–40°W): **a** averaged temperature time course for the austral winter seasons (July–September) from 1948 to 2007, **b** vertical profiles of winter sea water temperature averaged within three climate phases with the time frames specified in the plot, and **c** heat content, *Q*, within the upper 800-m layer for the period of 1948–2007

et al. 2007; Lee and McPhaden 2008; Swanson and Tsonis 2009; Wang et al. 2009; Akasofu 2010; Byshev et al. 2011) and indicates the global scale of the revealed ocean AUL heat content variability. Moreover, we suggest that this multi-decadal redistribution of the heat is a general feature of the Earth's climatic system, with heat discharge from specific large-scale ocean regions (Figs. 6, 7, 8, 9, 10) followed by warming over the adjacent continents (IPCC 2007; 2013).

The individual regional features of the water temperature variations in the North Atlantic Ocean (Fig. 6) and the North Pacific Ocean (Fig. 7) are also evident. In particular, the sea surface temperature (SST) during the second half of the 20th century changed much faster in the North Pacific than in the North Atlantic; however, in the latter, the AUL heat content underwent substantially more intense change

than in the former. These differences are likely related to deeper convection in the North Atlantic Ocean (up to the depths of 1000–1200 m), while stronger density stratification in the North Pacific Ocean prevents the convection development deeper than 500–600 m (Fig. 6 and 7). This result implies that the AUL heat content variations are a more reliable indicator of the heat transfer from the ocean into the atmosphere than the dynamics of the SST anomalies.

The numerically simulated MOHO characteristics can be compared with the observational data from the Russian MEGAPOLYGON program (Experiment MEGAPOLYGON 1992). The main purpose of this large-scale observation program, completed in 1987 in the North-Western Pacific Ocean, was to examine intense eddy formation in the region to the east of Japan, which is strongly affected by the Kuroshio and
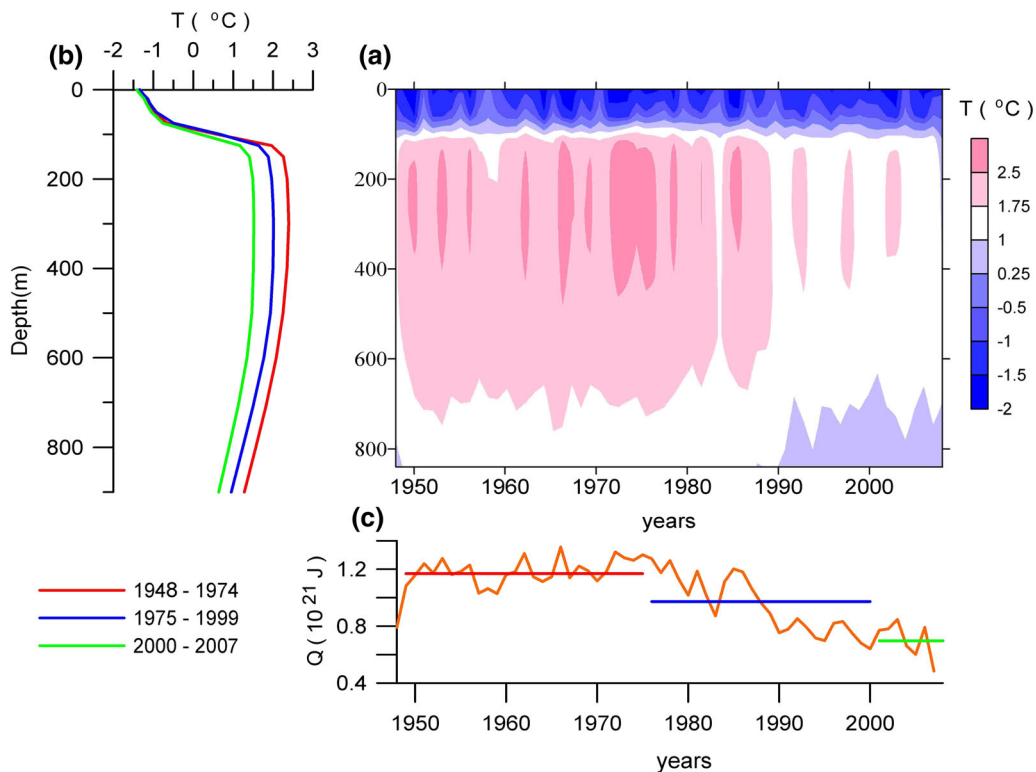
Figure 9
Same as in Fig. 8, but for the Southern IRO II (60°S–65°S, 72.5°E–77.5°E)

Kuril currents. This area corresponds with the Pacific IRO considered in the present study. Altogether, 11 Russian research vessels (r/v) worked in this region to fulfill the experiment program objectives. Over the period from May to November 1987, 177 moorings were simultaneously deployed with a typical interval of 20 nautical miles to continuously monitor the ocean currents, water temperature, salinity and meteorological characteristics. These moorings were supplemented by six water property surveys over the 600 by 600 km quadrangle area. The analysis of the MEGAPOLYGON data revealed that during the period of observations the oceanic heat budget within the study region was negative, while the heat flux from the ocean to the atmosphere increased by a factor of five compared to the climatic norm (Byshev and Snopkov 1990). Numerical experiments covering the MEGAPOLYGON time frame showed that the turbulent sensible and latent heat fluxes from the ocean to the atmosphere, as well as the effective ocean heat emission, significantly exceeded the total

heat influx to the ocean surface due mainly to short-wave solar radiation. The model revealed several additional indicators of the ocean surface cooling in the Pacific IRO, e.g., intensive cloud formation and anomalously low atmospheric pressure. All these observational results and their analysis are found in a good agreement with the results of our modeling studies of the water temperature evolution in the Pacific IRO (Figs. 4, 7).

The experiment ATLANTEX-90 in the north-western part of the Atlantic Ocean was led by the P.P. Shirshov Institute of Oceanology as part of the International Global Atmosphere Research Program (GARP). Three Russian ships, "Vityaz", "Academic Kurchatov" and "Professor Schtockman", were used in this observational program (Byshev et al. 1993). One of the main objectives of the experiment was to study the Newfoundland Climate-Active Zone during the period April to June, 1990. The field program included water property surveys, moored current measurements and meteorological observations.
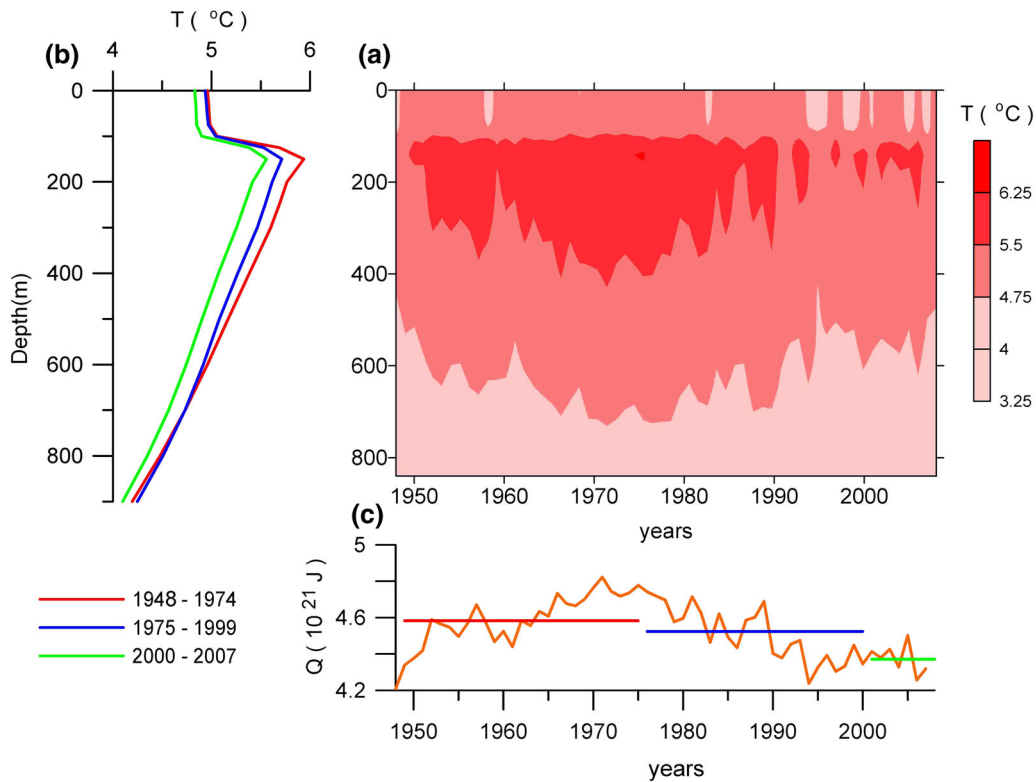
Figure 10
Same as in Fig. 8, but for the Southern IRO III (50°S–55°S, 145°E–150°E)

Analysis of the data showed that, during the experiment, the AUL in the area under study was anomalously cold from the surface to depths of 1000 m or more. Numerical model experiments done as part of the present study (Fig. 6) gave results which are in a good agreement with both of this observational program.

Overall, then the observational data from the MEGAPOLYGON and ATLANTEX-90 projects gave additional evidence of the formation of extensive temperature anomalies in the Pacific and Atlantic Oceans corresponding well with the climate warming over the continents. The model-simulated results have shown that the AUL heat discharge occurred in both hemispheres during the period from 1975 to 1999, that is, during the active phase of the modern climate warming over the continents. Specifics of this process in some of the areas, for example in the Southern IRO I [67.5°–62.5°S, 45°–40°W] (Fig. 8) and Southern IRO II [65°–60°S, 72.5°–77.5°E] (Fig. 9), was that the ocean heat has been transferred

to the sea surface from the warmer sub-surface layer (100–600 m depth), exclusively as a result of the deep convection. Note, that in such case, the process of the ocean heat loss can be disguised by development of a weak positive sea surface water temperature anomaly.

4. Conclusions

Based on the results of numerical modeling of temperature and salinity fields in the North Atlantic, North Pacific and Southern Oceans, we were able to reproduce the evolution of the ocean active upper layer (AUL) and identify the Multi-decadal Oscillation of the Heat content in the Ocean (MOHO). The model experiments for the five specific oceanic regions in these oceans showed that, at least within those areas, the MOHO can be described as alternating stages of the ocean heat accumulation and discharge with a typical periodicity of 25–35 years. We demonstrated that the
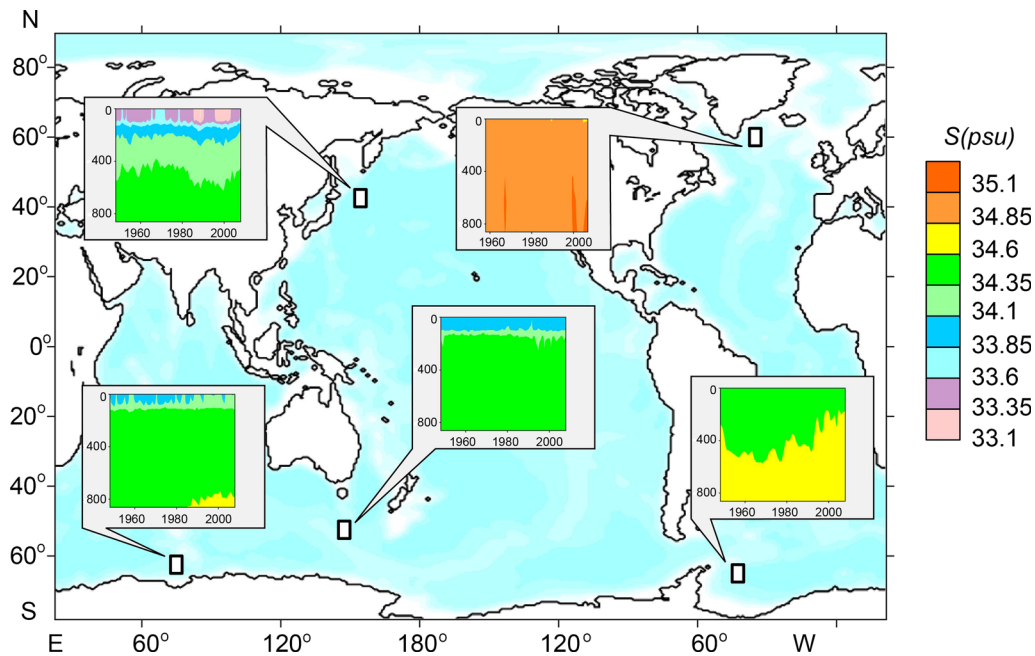
Figure 11
Simulated evolution of the AUL salinity structure in the five studied IRO. The *scales* on the *inset* axes: vertical-depth (m), horizontal-time (years)

AUL plays the role of a "rechargeable accumulator" with a feedback to the ocean/atmosphere system. Being superimposed on the major positive secular trend of the global ocean AUL heat content, the MOHO phases were found to coincide with the climate shifts on the adjacent continents.

The simulated long-term evolution of the oceanic upper layer exhibited heat loss within the studied energy-active areas during 1975–1999. This inherent process occurred concurrently with the continuous rise of the mean air temperature over the continents. Therefore, we assume that even the regional ocean forcing may be important for the development of the global-scale climatic processes. In this case, the climate over the land should become more "continental" during the MOHO phase, when the ocean AUL accumulates the heat from the atmosphere. In accordance with our present results, the MOHO was in this state before the mid-1970s and switched to this state once again at the beginning of this century (Byshev et al. 2006; Anisimov et al. 2012). This latest shift is also confirmed by the growth of the depth-averaged AUL temperature by as

much as 0.005 °C/year in the early 2000s as derived from the ARGO data (Roemich et al. 2015; Deabruyeres et al. 2016).

REFERENCES

Abraham, J. P., Baringer, M., Bindoff, N. L., et al. (2013). A review of global ocean temperature observations: Implications for ocean heat content estimates and climate change. *Reviews of Geophysics, 51,* 450–483. doi:10.1002/rog.20022.

Akasofu, S.-I. (2010). On the recovery from the Little Ice Age. *Natural Science, 2*(11), 1211–1224. doi:10.4236/ns.2010.211149.

Anisimov, M. V., Byshev, V. I., Zalesniy, V. B., & Moshonkin, S. N. (2012). Multi-decade variability of the North-Atlantic Ocean

thermal structure and its climate significance. *Doklady Earth Sciences, 443*(3), 372–376.

Atlas POLYMODE (1986), Woods Hole, USA.

Bond, N. A., Overland, J. E., Spillane, M., & Stabeno, P. (2003). Recent shifts in the state of the North Pacific. *Geophysical Research. Letters, 30*(23), 2183. doi:10.1029/2003GL018597.

Byshev, V. I., Figurkin, A. L., & Anisimov, I. M. (2016a). Recent climate change of thermohaline structure in the North West Pacific. *Izvestiya TINRO, 185,* 215–227.

Byshev, V. I., Koprova, L. I., Navrotskaya, S. E., Pozdnyakova, T. G., & Romanov, Yu A. (1993). Abnormal state of Newfoundland Energy Active Zone in 1990. *Doklady Earth Sciences, 331*(6), 735–738.

Byshev, V. I., Neiman, V. G., & Romanov, Yu A. (2006). On the essential differences between the large-scale variations of the surface temperature over oceans and continents. *Oceanology, 46*(2), 147–158.

Byshev, V. I., Neiman, V. G., Romanov, Yu A, & Serykh, I. V. (2009). On the spatial nonuniformity of some parameters of the global variations of the recent climate. *Doklady Earth Sciences, 426*(4), 705–709.

Byshev, V. I., Neiman, V. G., Romanov, Yu A, & Serykh, I. V. (2011). Phase variability of some characteristics of the present-day climate in the Northern Atlantic region. *Doklady Earth Sciences, 438*(2), 887–892.

Byshev, V. I., Neiman, V. G., Romanov, Yu A, Serykh, I. V., & Sonechkin, D. M. (2016b). Statistical significance and climatic role of the global atmospheric oscillation. *Oceanology, 56*(2), 165–171.

Byshev, V. I., & Orlov, V. S. (1993). Nature of intrathermocline lens on subpolar front in North Atlantic. *Oceanology, 33*(3), 293–298.

Byshev, V. I., & Snopkov, V. G. (1990). On surface temperature field forming in energy-active zone of the North-West Pacific Ocean in context of the MEGAPOLYGON Project. *Meteorology and Hydrology, 11,* 70–77.

Chambers, D. P., Merrifield, M. A., & Nerem, R. S. (2012). Is there a 60-year oscillation in global mean sea level? *Geophysical Research Letters, 39,* L18607. doi:10.1029/2012GL052885.

Chu, P. C. (2011). Global upper ocean heat content and climate variability. *Ocean Dynamics, 61,* 1189–1204. doi:10.1007/s10236-011-0411-x.

De Viron, O., Dickey, J. O., & Ghil, M. (2013). Global modes of climate variability. *Geophysical Research Letters, 40,* 1832–1837. doi:10.1002/grl.50386.

Deabruyeres, D., McDonagh, E. L., & King, B. A. (2016). Observational advances in estimates of oceanic heating. *Current Climate Change Reports, 2,* 127–134. doi:10.1007/s40641-016-0037-7.

Experiment MEGAPOLYGON. (1992). Hydro-physical study in the North-West Pacific Ocean Nauka, Moscow.

Gill, A. E. (1982). *Atmosphere-ocean dynamics, international geophysical series, 1982* (Vol. 30, p. 680). New York, London: Academic Press.

Gulev, S. K., & Latif, M. (2015). The origins of a climate oscillation. *Nature, 521,* 428–430. doi:10.1038/521428a.

Gulev, S. K., Latif, M., Park, W., Koltermann, K. P., & Keenlyside, N. (2013). North Atlantic Ocean control on surface heat flux on multi-decadal timescales. *Nature, 499,* 464–468. doi:10.1038/nature12268.

Gusev, A. V., & Dianskiy, N. A. (2014). Numerical simulation of the global ocean circulation and its climatic variability for 1948–2007 using INMOM, *Izvestiya. Atmospheric and. Oceanic Physics, 50*(1), 3–15.

IPCC. (2007). Climate Change: 2007. The physical science basis. In S. Solomon et al. (Eds.), *Contribution of WG1 to the IV assessment report of the IPCC*. Cambridge, UK and New York, NY, USA: Cambridge Univ. Press.

IPCC. (2013). Climate Change: 2013. The physical science basis. In T. F. Stocker et al. (Eds.), *Contribution of working group I to the fifth assessment report of the intergovernmental panel on climate change*. Cambridge, UK and New York, NY, USA: Cambridge University Press.

Ivanov, Yu. A., & Morozov, E. G. (1991). Water transport in Gulf Stream estuary. *Doklady Earth Sciences, 319*(2), 487–490.

Knight, J. R., Folland, C. K., & Scaife, A. A. (2006). Climate impacts of the Atlantic Multidecadal Oscillation. *Geophysical Research Letters, 33,* L17706. doi:10.1029/2006GL026242.

Kort, V. G., & Samoylenko, V. S. (Eds.). (1983). *Atlantic hydrophysical polygon-70* (p. 398). New Delhi: Oxonian Press PVT. Ltd.

Large, W. G., & Yager, S. G. (2004). *Diurnal to decadal global forcing for ocean and sea-ice models: the data sets and flu climatologies*. Boulder: Climate and Global Dynamics Division, National Center for Atmospheric Research.

Lebedev, S. A., & Kostianoy, A. G. (2008). Integrated using of satellite altimetry in investigation of meteorological, hydrological and hydrodynamic regime of the Caspian Sea. *Terrestrial Atmospheric and Oceanic Sciences, 19*(1–2), 71–82.

Lee, T., & McPhaden, M. J. (2008). Decadal phase change in large-scale sea level and winds in the Indo-Pacific region at the end of the 20-th Century. *Geophysical Research Letters, 35,* L01605. doi:10.1029/2007GL032419j.

Levitus, S., Antonov, J. I., Boyer, T. P., Locamini, R. A., & Garcia, H. E. (2009). Global ocean heat content 1955–2008 in light of recently revealed instrumentation problems. *Geophysical Research Letters, 36,* L07608. doi:10.1029/2008GL037155.

Li, S., & Luo, F. F. (2013). Lead-lag connection of the Atlantic Multidecadal Oscillation (AMO) with East Asian surface air temperatures in instrumental records. *Atmospheric and Oceanic Science Letters, 6*(3), 138–143.

Liman, J. M., Good, S. A., & Gouretski, V. V. (2010). Robust warming of the global upper ocean. *Nature*, 465, 334–337. doi:10.1038/nature09043.

Liu, P., & Sui, C.-H. (2014). An observational analysis of the oceanic and atmospheric structure of global-scale multi-decadal variability. *Advances Atmospheric Sciences, 31*(2), 316–330. doi:10.1007/s00376-013-2305-y.

Mann, M. E., Steinman, B. A., & Miller, S. K. (2014). On forced temperature changes, internal variability, and the AMO. *Geophysical Research Letters, 41,* 3211–3219. doi:10.1002/2014GL059233.

Minobe, S. A. (1997). 50–70 year climatic oscillation over the North Pacific and North America. *Geophysical Research Letters, 24,* 683–686.

Minobe, S. A. (1999). Resonance in bidecadal and pentadecadal climate oscillation over the North Pacific: Role in climatic regime shift. *Geophysical Research Letters, 26,* 855–858.

Mokhov, I. I., Semenov, V. A., Khon, V Ch., Latif, M., & Roeckner, E. (2008). Connection between Eurasia and North Atlantic climate anomalies and natural variations in the Atlantic thermohaline circulation based on long-term calculations. *Doklady Earth Sciencies, 419*(2), 502–505.

Monin, A. S. (1986). *An introduction to the theory of climate*. Dordrecht, The Netherlands: D. Reidel Publishing Company.

Moshonkin, S. N., Dianskiy, N. A., Eidinov, L. A., & Bagno, A. V. (2004). Coupled Northern Atlantic and Arctic Ocean circulation modeling. *Oceanology, 44*(6), 759–773.

Nakamura, M. (2013). Greenland sea surface temperature change and accompanying changes in the North Hemispheric climate. *Journal of Climate, 26,* 8576–8596. doi:10.1175/JCLI-D-12-00435.1.

Noake, K., Polson, D., Hegerl, G., & Zhang, X. (2012). Changes in seasonal land precipitation during the latter twentieth. *Geophysical Research Letters, 39,* L03706. doi:10.1029/2011GL050405.

Roemich, D., Church, J., Gilson, J., Monselesan, D., Sutton, P., & Wijffels, S. (2015). Unabated planetary warming and its ocean structure since 2006. *Nature climate change, 5,* 240–245.

Steinman, B. A., Mann, M. E., & Miller, S. K. (2015). Atlantic and Pacific multidecadal oscillations and Northern Hemisphere temperature. *Science, 347,* 988–991. doi:10.1126/science.1257856.

Stephens, C., Levitus, S., Antonov, J., & Boyer, T. P. (2001). On the Pacific Ocean regime shift. *Geophysical Research Letters, 28*(19), 3721–3724.

Swanson, K. L., & Tsonis, A. A. (2009). Has the climate recently shifted? *Geophysical Research Letters, 36,* L06711. doi:10.1029/2008GL037022.

Tsonis, A. A., Swanson, K., & Kravtsov, S. (2007). A new dynamical mechanism for major climate shifts. *Geophysical Research Letters, 34,* L13705. doi:10.1029/2007GL030288.

Wang, G., Swanson, K. L., & Tsonis, A. A. (2009). The pacemaker of major climate shifts. *Geophysical Research Letters, 36,* L07708. doi:10.1029/2008GL036874.

Watanabe, M., Kamae, Y., & Kimoto, M. (2014). Robust increase of the equatorial Pacific rainfall and its variability in a warmed climate. *Geophysical Research Letters, 41,* 3227–3232. doi:10.1002/2014GL059692.

World Ocean Database (2009). In: Levitus, S. (Ed.), NOAA Atlas NESDIS 66, U.S. Wash.: Gov. Printing Office, 215 p.

Wouters, B., Drijfhout, S., & Hazeleger, W. (2012). Interdecadal North-Atlantic meridional overturning circulation variability in EC-EARTH. *Climate Dynamics, 39,* 2695–2712. doi:10.1007/s00382-012-1366-4.

Wyatt, M. G., Kravtsov, S., & Tsonis, A. A. (2012). Atlantic multidecadal oscillation and Northern Hemispheres climate variability. *Climate Dynamics, 38,* 929–949. doi:10.1007/s00382-011-1071-8.

Zhang, L., Wang, C., & Wu, L. (2012). Low-frequency modulation of the Atlantic warm pool by the Atlantic multidecadal oscillation. *Climate Dynamics, 39,* 1661–1671. doi:10.1007/s00382-011-1257-0.